Towards quantitative electron holography of electrostatic potentials in doped semiconductors

P K Somodi, R E Dunin-Borkowski, A C Twitchett, C H W Barnes[1] and P A Midgley

Department of Materials Science and Metallurgy, University of Cambridge, Pembroke Street, Cambridge CB2 3QZ, UK
[1]Department of Physics, University of Cambridge, Madingley Road, Cambridge CB3 0HE, UK

ABSTRACT: Simulations of the electrostatic potential within thin Si samples containing an abrupt *p-n* junction have been compared with experimental measurements obtained using off-axis electron holography from samples prepared using focused ion beam milling. In order to obtain agreement between the simulated and experimental potential profiles, a layer of altered dopant concentration is introduced at the specimen surface.

1. INTRODUCTION

The quantitative characterisation of electrostatic potential distributions associated with the presence of dopant atoms is of fundamental importance for the development of future generations of nanoscale semiconductor structures and devices. Off-axis electron-holography (Völkl et al 1998) is increasingly used to determine the potential within doped semiconductors. However the step in potential across a *p-n* junction is usually found to be less than expected (Twitchett et al 2002, Rau et al 1999). This discrepancy has been partially accounted for by the introduction of equipotential surfaces on the specimen (Somodi et al 2004). Here we compare experimental electron holography results with two-dimensional simulations of the electrostatic potential across a *p-n* junction. In the simulations we introduce layers with altered dopant concentrations at the specimen surfaces to model the effect of sample preparation for electron microscopy on the electrostatic potential in a thin specimen.

2. COMPARISON OF EXPERIMENTAL AND SIMULATED RESULTS

Three Si *p-n* junction samples containing Sb atoms in the *n*-type regions and B atoms in the *p*-type regions were prepared for electron holography using focused ion beam (FIB) milling. Convergent beam electron diffraction was used to determine that the crystalline sample thicknesses were 220, 270 and 410 nm. The dopant concentrations were measured using secondary ion mass spectrometry (SIMS) and were found to be 3×10^{18} cm^{-3} in the *n*-type region and 4×10^{18} cm^{-3} in the *p*-type region. The potential distributions in the specimens were measured using electron holography as described elsewhere (Twitchett et al. 2004a). Figure 1 shows raw and smoothed potential profiles across the *p-n* junction measured from each specimen.

Simulations of the potential within the Si specimens were performed in one- and two- dimensions by solving the standard semiconductor equations (Sze 2002) and using a finite element solver (Langtangen 2003). The one-dimensional simulations give the expected bulk-like potential across the junction to be 1.04 V. In the two-dimensional simulations values for the electrostatic potential on the top and bottom surfaces are required. Experimentally, electrostatic fringing fields are almost never observed outside the specimen close to the position of a *p-n* junction (Twitchett 2004b) indicating that these surfaces can be treated as equipotentials for the purpose of the simulations. The simulated potential distributions were averaged in the direction of the electron beam in order to generate results that are comparable to those obtained using electron holography. It has been shown that the averaged step in potential across the junction is independent of the value of the potential at the surface for the dopant

concentrations considered here (Somodi et al 2004). Therefore the potential at the surface is taken to be 0.7eV above the Fermi level in bulk-like *n*-type silicon as suggested by Lűth (2001).

Figure 1 shows simulated potential profiles for all three specimen thicknesses. The step in potential across the junction that would be inferred from a knowledge of the sample thickness is found to be 0.4 V experimentally and 0.97 V for the simulations, for a sample thickness of 220 nm. For a sample thickness of 270 nm these values were 0.7 V experimentally and 0.98 V from the simulations while for the 410 nm thick sample the corresponding values are 0.75 V and 1.00 V. Although the inclusion of equipotentials on the specimen surface in the simulations act to reduce the apparent step in potential across the junction, as compared with the expected bulk-like value, it does not fully account for the observed decrease in the step in potential measured using electron holography.

A further discrepancy is associated with the fact that the depletion width across the junction is significantly larger in the experimental data than in the simulations. In the smoothed experimental data the depletion width is defined to be the region over which the gradient of the potential (i.e. the electric field) is non-zero. The depletion width is measured experimentally to be 65 ± 10, 90 ± 10 and 65 ± 10 nm for sample thicknesses of 220, 270 and 410 nm respectively. In the case of the simulations long tails present in the electric field distribution require the use of an alternative method to find the depletion width. In this case the depletion width is defined to be the distance over which the charge density is non-zero, assuming that the charge density takes values of either zero or the average dopant concentration within the specimen. The depletion width, calculated by integrating the charge density and from a knowledge of the maximum value of the electric field, is found to be 25 ± 5 nm for all three sample thicknesses. A one-dimensional simulation gives the expected depletion width across the junction to be 23 ± 1 nm. The introduction of equipotentials on the specimen surfaces clearly does not account for the increase in the depletion width observed in the microscope.
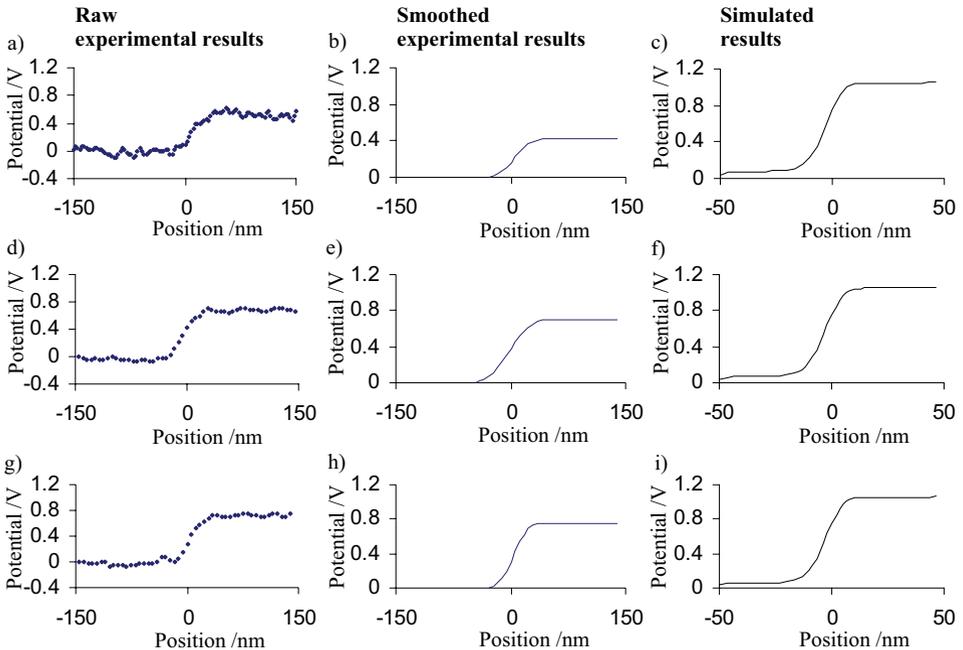

Fig. 1. The potential across a Si *p-n* junction doped with 3×10^{18} cm^{-3} of B in the *n*-type region and 4×10^{18} cm^{-3} of Sb in the *p*-type region. a), d) and g) show the raw experimental data from off-axis electron holography. b), e) and h) show the smoothed experimental data from which noise has been removed. c), f) and i) show simulated profiles. a), b) and c) are for samples of thickness 220 nm. d), e) and f) are for samples of thickness 270 nm. g), h) and i) are for samples of thickness 410 nm.

3. AN IMPROVED MODEL TO SHOW THE IMPACT OF FIB MILLING ON THE SILICON SURFACE

The experimentally observed decrease in the step in potential across the junction and increase in the depletion width are suggestive of a reduction in the electrically active dopant concentration in the sample. The dopant concentration measured using SIMS may not be the same as the electrically active concentration due to the effects of FIB milling on the sample. Here we model the effect of FIB milling on the potential within the sample by introducing a layer of lower dopant concentration on each surface of the sample as shown schematically in Fig. 2. The thickness of each layer d is varied, as is the dopant concentration in the layer.

The resulting simulated step in potential across the junction is shown as a function of d in Fig. 3, for the three sample thicknesses examined experimentally. It can be seen that the step in potential across the junction is further reduced by the introduction of surface layers of lower dopant concentration. Significantly, the reduction in the apparent step in potential is approximately independent of the dopant concentration in the surface layers, especially for smaller values of d. The corresponding variation in the simulated depletion width with surface layer thickness is shown in Fig. 4. The depletion width increases significantly with the introduction of surface layers and its value is approximately independent of the dopant concentration in the layers.
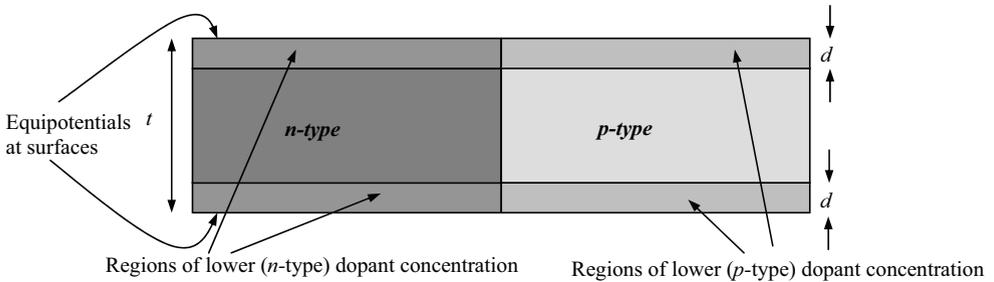

Fig. 2.   Schematic diagram showing the geometry of the sample assumed in the simulations, with modified surface layers to model the effect of FIB milling.
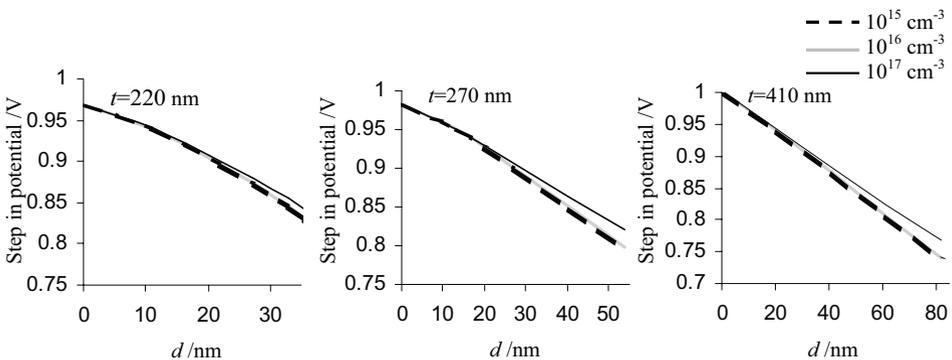

Fig. 3.   Graphs showing the simulated variation in potential across the junction with surface layer thickness, for the indicated sample thicknesses. The dopant concentrations on the surface were taken to be 10^{15}, 10^{16} and 10^{17} cm^{-3}.
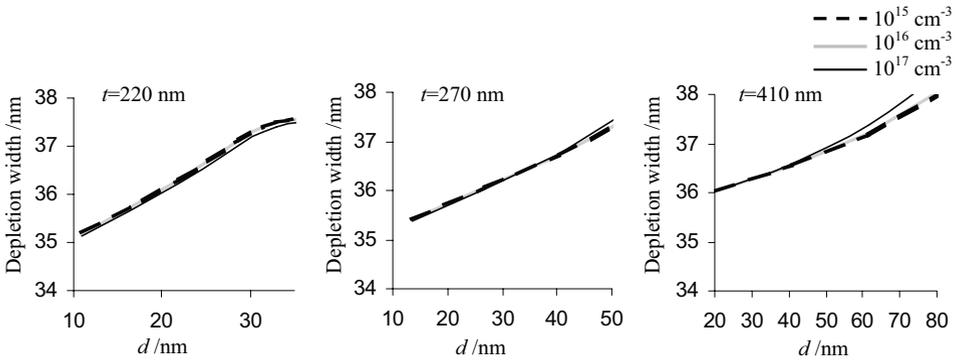
Fig. 4. Graphs showing the simulated variation in depletion width with surface layer thickness for the indicated sample thicknesses. The dopant concentrations in the surfaces layers are 10^{15}, 10^{16} and 10^{17} cm^{-3}.

The reduction in the step in potential across the junction seen in the experimental results, as compared with the value expected in bulk-like material, can be reproduced by these simulations. For larger sample thicknesses the surface layers of lower dopant concentration would need to account for almost half of the total sample thickness. For the smaller sample thicknesses the surface layers would have to dominate the sample. The larger depletion widths measured in the experimental data cannot be replicated in the present model. The discrepancy may be partially accounted for by the difficulty in measuring the depletion width. However it is more likely that the electrically active dopant concentrations in the centre of the sample are decreased from the nominal values measured using SIMS, in addition to the presence of altered surface layers.

4. CONCLUSIONS

It has been shown that the introduction of surface layers of lower dopant concentration in simulations decreases the potential across a *p-n* junction to values that are within agreement with values measured using electron holography. The large depletion widths measured using electron holography may be accounted for by a decrease in the electrically active dopant concentration throughout the thickness of the sample. These effects must be understood fully before electron holography can become a truly quantitative method to determine dopant profiles.

REFERENCES

Langtangen H P 2003 Computational Partial Differential Equations (London, Springer) ch 3
Lűth H 2001 Solid Surface, Interfaces and thin films, (Heidelberg, Springer) p 349
Rau W D, Schwander P, Baumann F H, Hoppner W and Ourmazd A 1999 Phys. Rev. Lett. **82,** 2614
Somodi P K, Dunin-Borkowski R E, Twitchett A C, Barnes C H W and Midgley P A 2004 Proc. XIII Eur. Congr. Microsc. II, p 387
Sze S M 2002 Semiconductor Devices (Singapore, Wiley) ch 4
Twitchett A C, Dunin-Borkowski R E and Midgley P A 2002 Phys. Rev. Lett. **88,** 238302
Twitchett A C, Dunin-Borkowski R E, Halifax R J, Broom R F and Midgley P A 2004a J. Microsc. **214**, p 287
Twitchett A C, Dunin-Borkowski R E, Halifax R J and Midgley P A 2004b J. Phys. Condens. Mat. **16**, S181
Völkl E, Allard L F and Joy D C 1998 Introduction to Electron Holography (New York, Kluwer Academic/ Plenum Publishers)